
This copy is for your personal, non-commercial use only.

If you wish to distribute this article to others, you can order high-quality copies for your colleagues, clients, or customers by [clicking here](#).

Permission to republish or repurpose articles or portions of articles can be obtained by following the guidelines [here](#).

The following resources related to this article are available online at www.sciencemag.org (this information is current as of October 17, 2014):

Updated information and services, including high-resolution figures, can be found in the online version of this article at:

<http://www.sciencemag.org/content/335/6073/1232>

Supporting Online Material can be found at:

<http://www.sciencemag.org/content/suppl/2012/02/09/science.1217869.DC1.html>

A list of selected additional articles on the Science Web sites **related to this article** can be found at:

<http://www.sciencemag.org/content/335/6073/1232#related>

This article **cites 42 articles**, 13 of which can be accessed free:

<http://www.sciencemag.org/content/335/6073/1232#ref-list-1>

This article has been **cited by** 12 articles hosted by HighWire Press; see:

<http://www.sciencemag.org/content/335/6073/1232#related-urls>

This article appears in the following **subject collections**:

Cell Biology

http://www.sciencemag.org/cgi/collection/cell_biol

Triggering a Cell Shape Change by Exploiting Preexisting Actomyosin Contractions

Minna Roh-Johnson,^{1*} Gidi Shemer,^{1*} Christopher D. Higgins,¹ Joseph H. McClellan,¹ Adam D. Werts,¹ U. Serdar Tulu,² Liang Gao,³ Eric Betzig,³ Daniel P. Kiehart,² Bob Goldstein^{1†}

Apical constriction changes cell shapes, driving critical morphogenetic events, including gastrulation in diverse organisms and neural tube closure in vertebrates. Apical constriction is thought to be triggered by contraction of apical actomyosin networks. We found that apical actomyosin contractions began before cell shape changes in both *Caenorhabditis elegans* and *Drosophila*. In *C. elegans*, actomyosin networks were initially dynamic, contracting and generating cortical tension without substantial shrinking of apical surfaces. Apical cell-cell contact zones and actomyosin only later moved increasingly in concert, with no detectable change in actomyosin dynamics or cortical tension. Thus, apical constriction appears to be triggered not by a change in cortical tension, but by dynamic linking of apical cell-cell contact zones to an already contractile apical cortex.

During development, dramatic rearrangements of cells and epithelia play key roles in shaping animals (1–4). Many rearrangements are driven by apical constriction, including neural tube closure (4), failure of which is a common human birth defect (5). Apical constric-

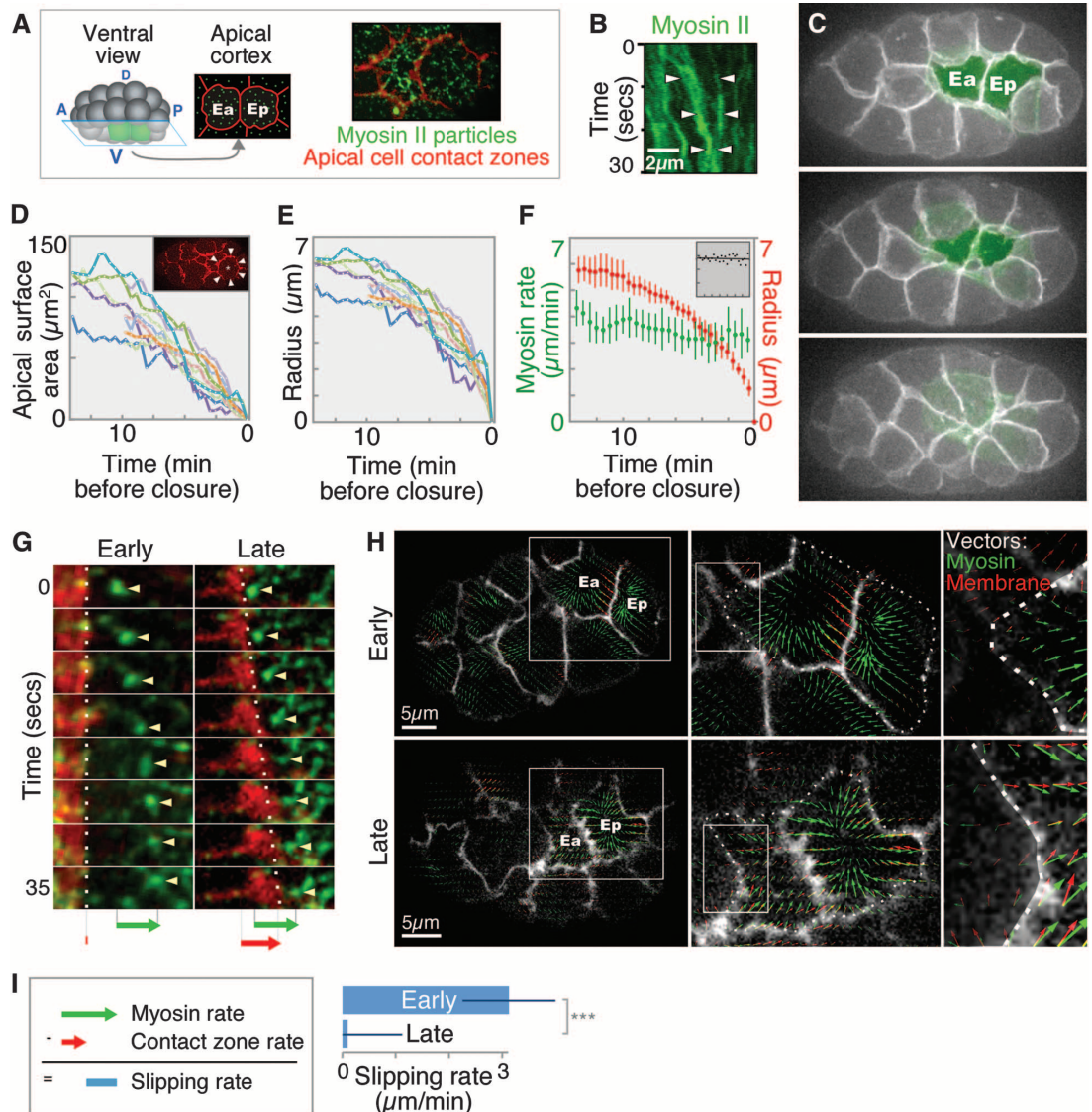
tion is generally driven by contraction of apical actomyosin networks (4). However, it is not well understood how the stresses and tensions generated by actomyosin networks produce cell shape changes in developing organisms (6).

To address this issue, we examined cortical actomyosin dynamics during *Caenorhabditis elegans* gastrulation. In *C. elegans*, two endodermal precursor cells (Ea and Ep) internalize through apical constriction (7–9). Transgenic green fluorescent protein (GFP) myosin II–containing particles formed in each cell’s apical cortex, enriched in Ea/p similarly to endogenous myosin (9). The ability to resolve large numbers of particles made it possible to track the detailed dynamics of ac-

¹Department of Biology, University of North Carolina at Chapel Hill, Chapel Hill, NC 27599, USA. ²Department of Biology, Duke University, Durham, NC 27708, USA. ³Janelia Farm Research Campus, Howard Hughes Medical Institute, Ashburn, VA 20147, USA.

*These authors contributed equally to this work. †To whom correspondence should be addressed. E-mail bobg@unc.edu

Fig. 1. Actomyosin contraction precedes the rapid shrinking of the apical surface. (A) Diagram of imaging method. (B) NMY-2::GFP coalescence (white arrowheads) in apical cortex of Ea/p cell. (C) Shrinking of apical surfaces during gastrulation (projections of 10 1- μ m z planes, with Ea/p false-colored). (D) Ea/p cell apical surface areas over 575 or 825 s (five embryos each) before closure of the apical surface. (Inset) Apical cell–cell contact zones (arrowheads) on Ep (asterisk). (E) Average radius of apical surfaces derived from area measurements. (F) Mean and 95% CI of radius and myosin particle rate over time. (Inset) Myosin directionality (net distance over total distance, vertical scale 0 to 1) over time (time scale: same as larger graph). (G) Movements of individual myosin particles (arrowheads) near contact zones (white dotted lines) in early or late stages of closure. Arrows at bottom indicate relative distances traveled by each. (H) PIV, three magnifications. Boxes indicate enlarged areas. Left to right are whole embryo at plane of Ea/p apical cortex, Ea/p cells (outlined by dotted line), and part of Ea at border with another cell. (I) Slipping rate calculated from individual particles and contact zones ($P < 0.001$, Student’s *t* test).



tomoyosin networks (Fig. 1A, fig. S1, and movie S1). Neighboring myosin particles moved short distances toward each other into multiple coalescence points, with most particles moving centripetally (toward the center of the apical cell surface) and with new particles forming near apical cell boundaries (Fig. 1B and fig. S2). These particles appear to be components of contracting actomyosin networks because F-actin coalesced similarly (fig. S2) and myosin particles near the center of each coalescence moved at a slower

speed than did those further away (fig. S3), as seen in other contracting actomyosin networks (10). Particle tracking and fluorescence recovery after photobleaching (FRAP) experiments suggested that the networks were continuously remodeled by exchange of myosin molecules on and off particles, as expected (fig. S3).

To investigate how apical actomyosin networks shrink apical cell surfaces, we tracked the outlines of these surfaces, the apical cell-cell contact zones, quantitatively (Fig. 1, C and D).

Apical areas shrunk gradually or not at all at first (Fig. 1, D and F) (11) and then accelerated. We predicted that actomyosin contraction would also begin gradually and accelerate in concert with the contact zones (Fig. 1E). Instead, myosin particles moved centripetally quite rapidly throughout this period [$3.19 \pm 0.14 \mu\text{m}/\text{min}$, mean \pm 95% confidence interval (CI)] (Fig. 1F), at first with little or no accompanying contact zone movement. Myosin particles near contact zones at first streamed away from the contact zones, which were in many

Fig. 2. Periodic actomyosin coalescence occurs before apical cell profiles shrink in *Drosophila* gastrulation. (A) *Drosophila* ventral furrow formation. Circles mark apical myosin enrichment seen before apical cell profiles began to shrink. (B) Kymograph of a cell (diagrammed) showing myosin (green) movement toward a stationary cell-cell boundary (red) before apical shrinking began. (C) Myosin coalesced (green arrowheads) and dissipated (gray arrowheads) before apical cell profiles began to shrink. This is shown quantitatively from one cell in (D) and from 11 cells chosen at random in (E). Heatmaps in (E) show local maxima of apical myosin levels (three-timepoint running averages of myosin level at each timepoint minus the average of 10 timepoints before and after, normalized to maximum and minimum). Green and gray arrowheads mark one case as in (C). Cell 3 is a rare example in which peaks were not seen before apical shrinking began. (F) Slipping rate, defined as in Fig. 1I, early (before apical shrinking, $n = 33$ cells, 3 embryos) and late (during apical shrinking, $n = 27$ cells, 3 embryos), $P < 0.01$ (Student's t test).

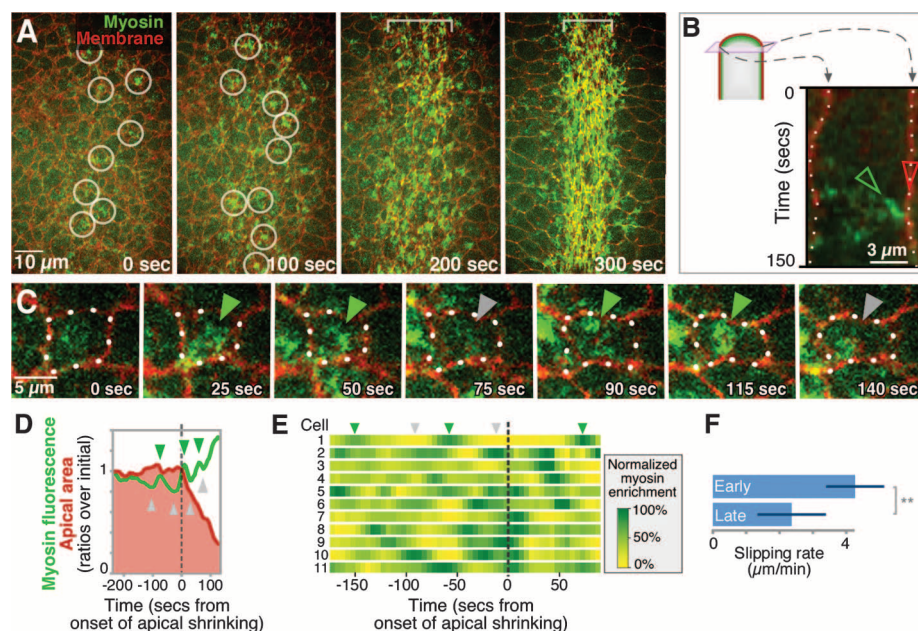
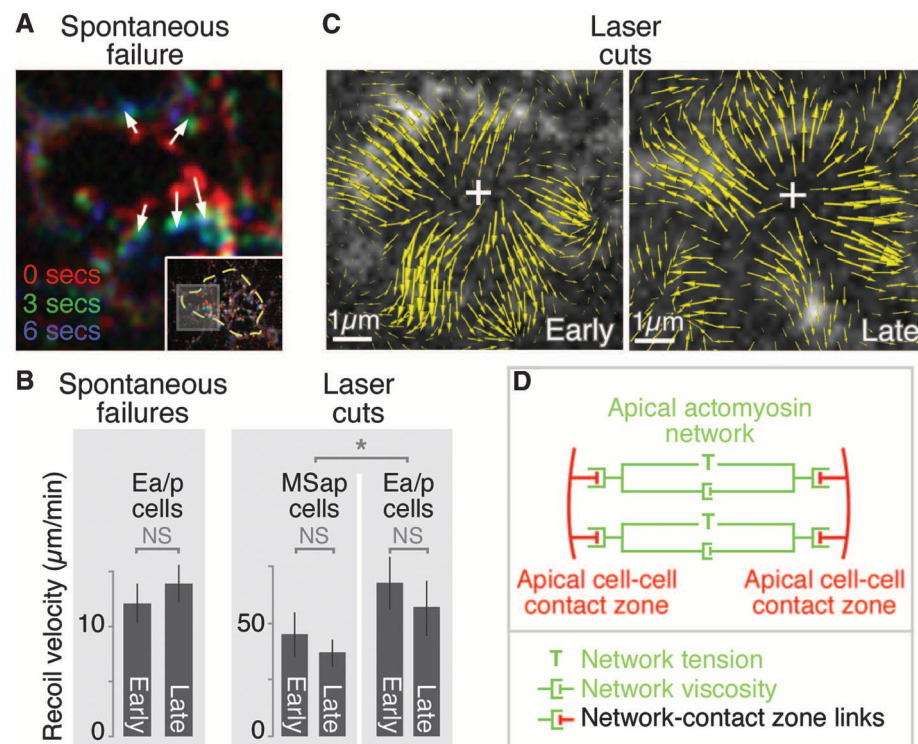


Fig. 3. Cortical tension associated with apical constriction is established early and changes little as apical shrinking accelerates in *C. elegans*. (A) A spontaneous failure, with three timepoints overlain in three colors. (Inset) Entire Ea/p cell apical cortex outlined with enlarged region indicated. Arrows mark individual myosin particles springing apart. (B) Similar data from Ea/p cortical laser cuts done in early or late stages by means of PIV as in Fig. 1H. (C) Initial recoil speeds of myosin particles after spontaneous failures at early ($n = 13$ myosin particles within $1 \mu\text{m}$ of center of recoil, six embryos) and late (20 particles, seven embryos) stages, or after laser cuts (48 particles within $4 \mu\text{m}$ of cut site, seven embryos per stage). Exponential decay $T_{1/2}$ was 2.20 s in early stages, $n = 12$ particles; 2.38 s in late stages, $n = 20$ particles. (D) Working model of forces acting on contact zones (red) and within Ea/p apical actomyosin networks (green, with multiple, interconnected network elements represented as two elements here for simplicity). Results suggest that cortical tension (T) and network stiffness or viscous drag (green dashpots) within Ea/p change little from early to late stages.



cases almost stationary, suggesting that the actomyosin network and contact zones were only weakly mechanically connected at this stage (we refer to actomyosin contractions without contact zone movement as uncoupled movements) (Fig. 1G and movies S2 and S3). Later, contact zones appeared to move almost in unison with many of the myosin particles (referred to as coupled movements) (Fig. 1G and movie S4), suggesting that the myosin and contact zones may have become mechanically connected. Contact zones were never seen to overtake myosin particles in the Ea/p cortex (movies S2 to S5), suggesting that neighboring cells were not simply migrating over Ea/p cells.

Our observations were not entirely consistent with a simple pattern of uncoupled movements early and coupled movements later (fig. S4); instead, some variation existed at each stage. Tracking movements by means of particle image velocimetry (PIV) demonstrated that in general, the myosin particles and contact zones moved increasingly in unison as time progressed (Fig. 1H). We confirmed this result by measuring the rates of individually tracked myosin particles and nearby contact zones, defining the difference between these two rates as a slipping rate (Fig. 1I). Actomyosin contractions appeared to drive contact zone movements with ~25% efficiency in early stages, increasing to ~81% efficiency near the end of Ea/p internalization, based on comparison of measurements from cells with a computer simulation (fig. S5 and movie S6). Labeling cell surfaces with quantum dots or a plasma membrane marker demonstrated that cell surfaces moved in concert with underlying actomyosin network contractions—there may be strong frictional force or drag force between the actomyosin network and the overlying plasma membrane (fig. S6). Thus, slipping between actomyosin and membrane occurred specifically at apical cell contact zones, and the relationship between cytoskeletal dynamics and cell shape change during apical constriction is more dynamic than existing models (3, 4) predict.

To determine whether the phenomenon we found is conserved in other systems, we examined *Drosophila* ventral furrow cells (11), in which periodic actomyosin contractions cause apical cross-sectional profiles to shrink in pulses (12). We noticed myosin accumulations in some cells even before shrinking of apical profiles began (Fig. 2A). Myosin coalesced and moved either toward or away from stationary membranes and thus was not well connected to contact zone movements at first (Fig. 2B and movie S7). One or more rounds of myosin enrichment and dissipation occurred in most cells (89%; $n = 55$ cells) before apical profiles began to shrink (Fig. 2, C to E). These early actomyosin contractions occurred periodically, with a time interval of 75 ± 24 s, which is similar to that previously measured just after this stage, during apical constriction (12). Some of the early contractions might contribute to cell surface flattening in *Drosophila* because apical surfaces are not yet completely flattened at this stage (13), although many early contractions were not centripetally directed (Fig. 2B). Myosin moved at a faster rate than did nearby contact zones at first, and this difference was significantly reduced later, as also observed in *C. elegans* (Fig. 2F). Thus, the early activation of actomyosin contraction, before apical cell profiles begin to shrink, might be a conserved feature of apical constriction.

We hypothesized that a change in the apparent efficiency of actomyosin-contact zone connections suggested by our *C. elegans* results might be a secondary effect of changes in viscoelastic properties—for example, stiffening or softening of actomyosin networks in contracting cells or their neighbors. We tested this in two ways. First, we analyzed a naturally occurring phenomenon. The apical networks in Ea/p cells occasionally failed spontaneously, with centripetally moving myosin particles suddenly springing away from one another (Fig. 3A). During recoil, myosin particle movements slowed exponentially, suggesting that the apical cortex behaves as a viscoelastic network (14–16), and initial recoil speeds and their exponential decays were similar be-

tween early and late stages, suggesting little change in cortical tension or stiffness of the network over time (Fig. 3B) (15, 17). Second, we cut the cortical actomyosin network using a focused ultraviolet laser beam and measured initial recoil speed as a quantitative estimate of tension in the network (18–23). The cortical network recoiled rapidly from cuts in Ea/p (Fig. 3, B and C), again with little change in initial recoil speed between early and late stages (Fig. 3B). Cutting a neighboring cell's cortex produced a recoil that also did not change significantly over time, and that was slower than in Ea/p (Fig. 3B), suggesting that network tension is lower in this cell. Thus, the large difference in the degree of coupled movement between early and late stages is accompanied by little measurable difference in the viscoelastic properties of cortical networks. These results reveal that the cortical tension associated with apical constriction (Fig. 3D) is established well before apical constriction begins and suggest that the differences between early and late stages might be explained by a change in efficiency of actomyosin-contact zone connections alone.

These results support a picture in which a continuously coalescing apical actomyosin network adds little cortical tension as it begins to move apical cell-contact zones; the tension involved in coalescing the apical actomyosin network is great compared with the small additional tension required to pull contact zones. Although this model may appear counterintuitive, it is in fact consistent with estimates of forces in other biological systems on this size scale (19, 24).

Our results build a model of apical constriction in which the relevant cytoskeletal dynamics can run constitutively, transitioning to driving rapid cell shape change at a later time. We speculate that there may exist in this system a molecular clutch—a regulatable, molecular connection between actomyosin networks and contact zones, transmitting the forces generated by actomyosin contraction to the contact zones. Molecular clutches coordinate actin dynamics and adhe-

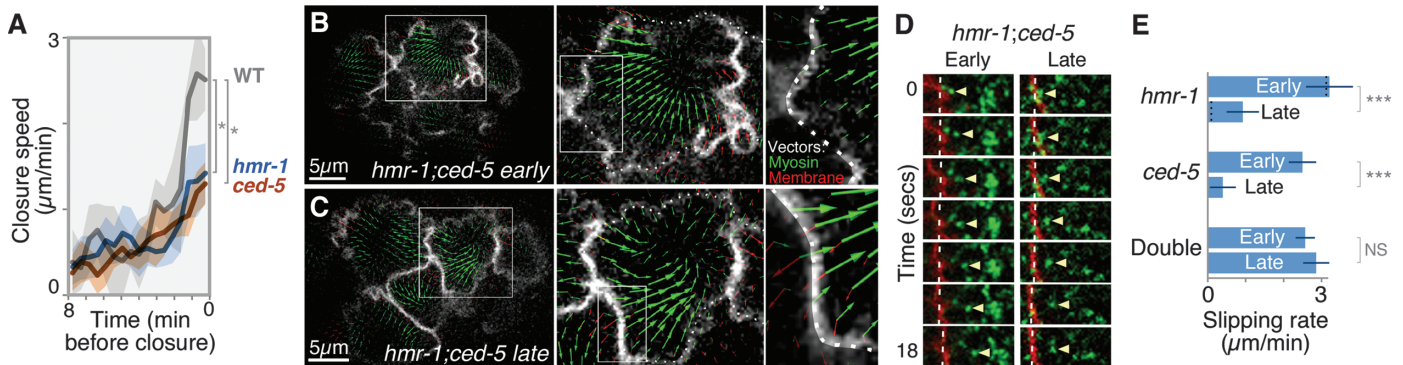


Fig. 4. Targeting classical cadherin and Rac signaling prevents coupled movements but not actomyosin contraction. (A) Closure speed (micrometer-per-minute decrease in average diameter) of apical cell areas in *hmr-1(RNAi)* or *ced-5(n1812)* does not reach the speed found in wild-type embryos (* $P < 0.05$). (B and C) PIV in

hmr-1(RNAi);ced-5(n1812) doubles. Myosin moves centripetally with little membrane movement in the same direction at either stage. This is shown for individual particles in (D), with quantification as in Fig. 1I in (E). Black dotted lines on *hmr-1* bars in (E) mark wild type for comparison. *** $P < 0.001$ (Student's t test).

sion formation in migrating growth cones and cultured cells (25). Our results raise the possibility that there might be developmentally regulated clutches functioning in epithelial morphogenesis. Indeed, targeting a cadherin-catenin complex and a Rac pathway prevented the transition to coupled movements, genetically separating coupled movements from contractions in this system (Fig. 4 and figs. S7 to S9). Thus, cadherin-catenin complex members, Rac pathway targets, or proteins that function alongside either might contribute to a clutch. Temporal regulation of actin nucleators at contact zones could also function as a clutch, if actin polymerized in a centripetal direction from contact zones primarily at early stages. In either model, gradual engagement of a clutch would stabilize connections between a contracting actomyosin network and cell-cell boundaries. Alternatively, resistance to a slipping clutch could change over time—for example, because neighboring cells lose tension. This alternative appears unlikely because we detected no change in neighboring cell tension over time. Instead, we speculate that the degree of engagement of a molecular clutch might determine the rate of apical shrinking. As apical shrinking proceeds, this rate might be limited additionally by the rate at which apical membrane can be removed (26).

Recent work has highlighted a number of actomyosin-based mechanisms that drive cell shape changes in morphogenesis (21, 27, 28). Periodic contractions of actomyosin networks, flows of actomyosin, and an actomyosin-based ratchet make contributions to changing cell shapes (12, 23, 29, 30). We found that the actomyosin

contractions and cortical tension associated with a cell shape change are established even before the cell shape change begins. Thus, the immediate trigger for apical constriction is not the activation of actomyosin contractions or a change in cortical tension, suggesting a role for the dynamic connections between the actomyosin cytoskeleton and the sites of cell-cell adhesion in morphogenesis mechanisms.

References and Notes

1. P. Friedl, D. Gilmour, *Nat. Rev. Mol. Cell Biol.* **10**, 445 (2009).
2. C. J. Weijer, *J. Cell Sci.* **122**, 3215 (2009).
3. G. M. Odell, G. Oster, P. Alberch, B. Burnside, *Dev. Biol.* **85**, 446 (1981).
4. J. M. Sawyer *et al.*, *Dev. Biol.* **341**, 5 (2010).
5. A. J. Copp, N. D. Greene, *J. Pathol.* **220**, 217 (2010).
6. S. W. Grill, *Curr. Opin. Genet. Dev.* **21**, 647 (2011).
7. J. Y. Lee, B. Goldstein, *Development* **130**, 307 (2003).
8. J. Y. Lee *et al.*, *Curr. Biol.* **16**, 1986 (2006).
9. J. Nance, J. R. Priess, *Development* **129**, 387 (2002).
10. E. Munro, J. Nance, J. R. Priess, *Dev. Cell* **7**, 413 (2004).
11. Materials and methods are available as supporting material on Science Online
12. A. C. Martin, M. Kaschube, E. F. Wieschaus, *Nature* **457**, 495 (2009).
13. R. E. Dawes-Hoang *et al.*, *Development* **132**, 4165 (2005).
14. B. Fabry *et al.*, *Phys. Rev. Lett.* **87**, 148102 (2001).
15. M. Mayer, M. Depken, J. S. Bois, F. Jülicher, S. W. Grill, *Nature* **467**, 617 (2010).
16. F. Wottawah *et al.*, *Phys. Rev. Lett.* **94**, 098103 (2005).
17. Y. Toyama, X. G. Peralta, A. R. Wells, D. P. Kiehart, G. S. Edwards, *Science* **321**, 1683 (2008).
18. R. Fernandez-Gonzalez, S. M. Simoes, J. C. Röper, S. Eaton, J. A. Zallen, *Dev. Cell* **17**, 736 (2009).
19. M. S. Hutson *et al.*, *Science* **300**, 145 (2003).
20. D. P. Kiehart, C. G. Galbraith, K. A. Edwards, W. L. Rickoll, R. A. Montague, *J. Cell Biol.* **149**, 471 (2000).

21. A. C. Martin, M. Gelbart, R. Fernandez-Gonzalez, M. Kaschube, E. F. Wieschaus, *J. Cell Biol.* **188**, 735 (2010).
22. M. Rauzi, P. Verant, T. Lecuit, P. F. Lenne, *Nat. Cell Biol.* **10**, 1401 (2008).
23. J. Solon, A. Kaya-Copur, J. Colombelli, D. Brunner, *Cell* **137**, 1331 (2009).
24. S. W. Grill, P. Gönczy, E. H. Stelzer, A. A. Hyman, *Nature* **409**, 630 (2001).
25. T. Mitchison, M. Kirschner, *Neuron* **1**, 761 (1988).
26. J. Y. Lee, R. M. Harland, *Curr. Biol.* **20**, 253 (2010).
27. K. E. Kasza, J. A. Zallen, *Curr. Opin. Cell Biol.* **23**, 30 (2011).
28. T. Lecuit, P. F. Lenne, E. Munro, *Annu. Rev. Cell Dev. Biol.* **27**, 157 (2011).
29. L. He, X. Wang, H. L. Tang, D. J. Montell, *Nat. Cell Biol.* **12**, 1133 (2010).
30. M. Rauzi, P. F. Lenne, T. Lecuit, *Nature* **468**, 1110 (2010).

Acknowledgments: We thank K. Bloom, G. Edwards, J. Iwasa, J. Johnson, E. Munro, M. Peifer, D. Reiner, S. Rogers, and members of the Goldstein lab for comments on the manuscript; B. Eastwood and R. Taylor for help with particle image velocimetry; J. Fricks for help with statistical analysis; and A. Martin and E. Wieschaus for providing fly strains and sharing movies. This work was supported by NIH R01 GM083071 to B.G., NIH R01 GM33830 to D.P.K., and a Human Frontier Science Program postdoctoral fellowship to G.S. Data reported in this paper are presented in the main paper and in the supporting online material. U.S. patent application no. 13/160,492 concerning Bessel beam plane illumination microscopy has been filed by the Howard Hughes Medical Institute on behalf of E.B.

Supporting Online Material

www.sciencemag.org/cgi/content/full/science.1217869/DC1
Materials and Methods
Figs. S1 to S11
Table S1
References (31–43)
Movies S1 to S8

13 December 2011; accepted 27 January 2012
Published online 9 February 2012;
10.1126/science.1217869

Nucleosomes Suppress Spontaneous Mutations Base-Specifically in Eukaryotes

Xiaoshu Chen,^{1,2} Zhidong Chen,¹ Han Chen,¹ Zhijian Su,^{1,3} Jianfeng Yang,¹ Fangqin Lin,¹ Suhua Shi,¹ Xionglei He^{1,2*}

It is unknown how the composition and structure of DNA within the cell affect spontaneous mutations. Theory suggests that in eukaryotic genomes, nucleosomal DNA undergoes fewer C→T mutations because of suppressed cytosine hydrolytic deamination relative to nucleosome-depleted DNA. Comparative genomic analyses and a mutation accumulation experiment showed that nucleosome occupancy nearly eliminated cytosine deamination, resulting in an ~50% decrease of the C→T mutation rate in nucleosomal DNA. Furthermore, the rates of G→T and A→T mutations were also about twofold suppressed by nucleosomes. On the basis of these results, we conclude that nucleosome-dependent mutation spectra affect eukaryotic genome structure and evolution and may have implications for understanding the origin of mutations in cancers and in induced pluripotent stem cells.

The mutation rates and spectra of adenine, thymine, cytosine, and guanine vary among the four bases that constitute DNA (1–3). In particular, cytosine is subject to a high rate of hydrolytic deamination, which is a major

source of C→T mutations (4). DNA melting is a rate-limiting step for cytosine hydrolytic deamination, because only when DNA is in its single-stranded form are both the N-3 and C-4 positions of the cytosine base subject to chem-

ical changes mediated by water (5). Due to ambient thermal fluctuations, a DNA double helix can spontaneously denature in local regions under normal physiological conditions within a cell, producing transient single-stranded DNA bubbles (6), a phenomenon called “DNA breathing.” Most eukaryotic genomic DNA is packed into nucleosomes, structural units of chromatin composed of ~147 base pairs (bp) of DNA wrapped around a histone octamer and connected by ~20 to 40 bp of unwrapped linker DNA (7). DNA packed into nucleosomes may be more resistant to DNA breathing, and therefore subject to less cytosine deamination, than the naked DNA found in nucleosome-depleted regions (8).

¹State Key Laboratory of Bio-control, College of Life Sciences, Sun Yat-sen University, Guangzhou 510275, China. ²The Key Laboratory of Gene Engineering of Ministry of Education, College of Life Sciences, Sun Yat-sen University, Guangzhou 510275, China. ³Gungdong Provincial Key Laboratory of Bio-engineering Medicine, Jinan University, Guangzhou 510632, China.

*To whom correspondence should be addressed at 135, Xingang West, College of Life Sciences, Sun Yat-sen University, Guangzhou 510275, China. E-mail: hexiongli@mail.sysu.edu.cn